

Signature of the interaction between dark energy and dark matter in observations

Elcio Abdalla,^{*} L. Raul Abramo,[†] and José C. C. de Souza[‡]

*Instituto de Física, Universidade de São Paulo,
C.P. 66318, 05315-970, São Paulo, SP, Brazil*

Abstract

We investigate the effect of an interaction between dark energy and dark matter upon the dynamics of galaxy clusters. This effect is computed through the Layser-Irvine equation, which describes how an astrophysical system reaches virial equilibrium and was modified to include the dark interactions. Using observational data from almost 100 purportedly relaxed galaxy clusters we put constraints on the strength of the couplings in the dark sector. We compare our results with those from other observations and find that a positive (in the sense of energy flow from dark energy to dark matter) non vanishing interaction is consistent with the data within several standard deviations.

PACS numbers: 98.80.C9; 98.80.-k

^{*}Electronic address: eabdalla@fma.if.usp.br

[†]Electronic address: abramo@fma.if.usp.br

[‡]Electronic address: jccampos@fma.if.usp.br

I. INTRODUCTION

One of the most surprising results of physics and cosmology in the last ten years is the cosmological accelerated expansion, which has been proved beyond reasonable doubt by observations [1–3]. The simplest explanation of such observations is a cosmological constant, which is, however, off theoretical computations by 120 orders of magnitude, a result that calls for urgent explanations. Another possibility is to argue that the Universe contains a strange dynamical component with negative pressure, dark energy, which is responsible for more than three quarters of its energy content [4].

Interactions of dark energy or dark matter with baryonic matter and radiation must be either inexistent or negligible in order to comply with stringent observations of the visible sector. However, in a field-theoretical approach, dark matter is some particle of a unification scheme, and dark energy should also be described by a field, which means that some level of interaction between these different sectors is basically mandatory. In the literature there is a large body of work dealing with such a possibility, e.g., [5]–[14]. It is interesting to notice that a coupling between dark energy and dark matter can also serve to alleviate the coincidence problem [5, 11]. The value of the coupling and holographic arguments also allow for the crossing of the phantom barrier which separates models with equations of state $w \equiv p/\rho > -1$ from models with $w < -1$ [12] – see also [14, 15]. Further consequences of the interaction have been studied, as *e.g.* its effect on the lowest multipoles of the cosmic microwave background (CMB) spectrum [13, 16]. The strength of the coupling is presumably as small as the fine structure constant [13, 17]. Comparison with supernova data and CMB and large-scale structure have also been analysed [18]. Nevertheless, the observational limits on the strength of such an interaction remain weak [19].

In addition to these constraints, dynamical dark energy (i.e., a time- and space-dependent field) has an impact on the large-scale structure due to its fluctuations. In that case, dark energy affects the process of structure formation by means of its density fluctuations, both in the linear [11], [20]–[23] and the non-linear [24, 25] regimes, as the growth of dark matter perturbations can be affected [13, 14, 26].

However, most constraints on dark interactions concern the asymptotic behaviour of the dark sector, both in time and in space. Local or nearby checks are still weak. This started to change with the detailed analysis of galaxy clusters and their internal structure. It was suggested that the dynamical equilibrium of collapsed structures could be affected by the coupling of dark energy to dark matter, which as a result could affect the averaged energy distributions predicted by the

virial theorem – in fact, by its relativistic counterpart, the Layser-Irvine equation [27]. This was first proposed, and analyzed for the Abell cluster A586, by [28]. The basic idea is that the virial theorem is distorted by the mass non-conservation generated by the coupling of dark matter with dark energy.

In a previous paper [29] we showed how the Layser-Irvine equation, describing the evolution towards virialization, is changed by the presence of the coupling. We showed that this violation leads to a systematic bias in the estimation of virial masses of clusters when the usual virial conditions are employed. By comparing weak lensing and X-ray mass-observables on the one hand, and virial masses on the other hand, we were able to cross-check not only the strength of the coupling, but also whether it was indeed a feature of the virial mass estimate, and not a more complicated set of biases between all these mass-observable relations. Our main result was that a single parameter could explain all the bias between virial mass and the other estimates (weak lensing and X-ray) to 95% confidence level (C.L.), or, equivalently, two standard deviations.

However, the amount of data (about thirty independent useful observations) did not allow a detailed numerical analysis, resulting in relatively weak constraints on the coupling. In this paper we will not only reanalyze that data, but will also include a new set of data for almost a hundred X-ray observations of galaxy clusters, and compare the presumed mass from those observations with the virial masses for those clusters.

Notice that even though the uncertainties associated with any individual galaxy cluster are very large, by comparing the naive virial masses of a large sample of clusters with their masses estimated by X-ray and by weak lensing data, we are able to constrain the bias between them and to impose much tighter limits on the strength of the coupling than has been achieved before.

II. PHENOMENOLOGY OF COUPLED DARK ENERGY AND DARK MATTER MODELS

We start with a simplified two fluid model interaction:

$$\begin{aligned}\dot{\rho}_{dm} + 3H\rho_{dm} &= \psi \\ \dot{\rho}_{de} + 3H\rho_{de}(1 + w_{de}) &= -\psi ,\end{aligned}\tag{1}$$

where a dot denotes time derivative, H is the expansion rate, ρ_{dm} and ρ_{de} are respectively the energy densities of dark matter and dark energy, and w_{dm} and w_{de} are their equations of state. Notice that the continuity equation still holds for the total energy density $\rho_{Tot} = \rho_{dm} + \rho_{de}$.

Phenomenologically, one can describe the interaction between the two fluids as an exchange of energy at a rate proportional to a combination of the energy densities [9, 12]:

$$\psi = \zeta H \rho_{Tot} . \quad (2)$$

In fact, the term proportional to ρ_{dm} could lead to instabilities [30, 31], but that does not concern us here in view of the local character of the computation. We are interested in collapsed structures where the local, inhomogeneous density σ is far from the average, homogeneous density ρ . In that case the continuity equation for dark matter reads [25]:

$$\dot{\sigma}_{dm} + 3H\sigma_{dm} + \vec{\nabla}(\sigma_{dm}\vec{v}_{dm}) = \zeta H(\sigma_{dm} + \sigma_{de}) , \quad (3)$$

where \vec{v}_{dm} is the peculiar velocity of dark matter particles. We have considered the local density of dark energy to be proportional to the local density of dark matter, $\sigma_{de} = b_{em}\sigma_{dm}$. If for a given model the dark energy component is very homogeneous, then $b_{em} \approx 0$. We do not consider the case where b_{em} depends on the size and mass of the collapsed structure – although this should probably happen in realistic models of structure formation with dark energy [25]. Hence, the continuity equation with dark matter coupled to dark energy reads:

$$\dot{\sigma}_{dm} + 3H\sigma_{dm} + \vec{\nabla}(\sigma_{dm}\vec{v}_{dm}) = \bar{\zeta} H \sigma_{dm} , \quad (4)$$

where $\bar{\zeta} = \zeta(1 + b_{em})$.

Considering that the kinetic (K_{dm}) and potential (U_{dm}) energies of a set of particles interact via gravity and the coupling (2), we found that the corrected Layser-Irvine equation leads to the condition:

$$(2 - \bar{\zeta})K_{dm} + (1 + b_{em})(1 - 2\bar{\zeta})U_{dm} = 0 . \quad (5)$$

Taking $\bar{\zeta} = b_{em} = 0$ we recover the usual virial condition.

III. MASS ESTIMATION AND LIMITS ON THE COUPLING

In order to find deviations from the virial theorem we analyse galaxy clusters, which are the largest virialized structures in the Universe [32, 33]. Studies of cluster in the optical, in X-ray and through weak lensing are available in the literature, which can then be used to estimate the mass of the cluster, under some hypotheses.

Clusters can be observed directly in the optical wavelengths, where the radial velocities are estimated through their projected (line-of-sight) velocities. The velocity field, together with the

projected spatial distribution of galaxies in the cluster, allow for an estimate of the relative shares of the potential and kinetic energy of its constituents. Assuming that the clusters are virialized, their masses can then be computed. But if there is a coupling of dark energy to dark matter, we find that [29]

$$(1 + b_{em}) \frac{U_{dm}}{K_{dm}} = -2 \frac{1 - \bar{\zeta}/2}{1 - 2\bar{\zeta}}. \quad (6)$$

Since the potential energy is proportional to the square of the masses, and the kinetic energy is only linearly proportional to the mass, there is a shift in the usual virial mass estimation, which is entirely due to the coupling, by a factor of $(1 - 2\bar{\zeta})/(1 - \bar{\zeta}/2)$.

One can measure the mass with other observations by making very simple assumptions which have nothing to do with the precise nature of the equilibrium of the system. In particular, both the weak lensing and X-ray methods provide physical observables which can be used to estimate the total mass of a cluster in ways which are totally independent of the virial method.

In what follows we will assume that the variations in the mass estimators can be explained by a single parameter – the coupling between dark energy and dark matter. Of course, all these mass estimates are rife with systematic errors of many types, and intrinsic uncertainties in these estimates should be expected. For instance, if the gas in a cluster is not homogeneously distributed, the clumps of gas will enhance the X-ray luminosity of the cluster relative to a homogeneous distribution (as the X-ray luminosity is proportional to the square of the number density of free electrons), leading to a possible overestimation of the X-ray mass. Clearly, our method cannot make a distinction between the constraint on the coupling of the dark sector and some other source of systematic error, such as the clumpiness of gas in clusters.

We parametrize this single-parameter deviation in mass estimations, both with weak lensing or X-ray data, as:

$$M_{vir} = \frac{1 - \bar{\zeta}/2}{1 - 2\bar{\zeta}} M_X = \frac{1 - \bar{\zeta}/2}{1 - 2\bar{\zeta}} M_{WL} \quad (7)$$

Previously [29], we compared and cross-checked the three ratios that can be obtained from each pair of masses. We obtained that $\zeta = 0.04 \pm 0.02$, and checked that there was no bias between X-ray and weak lensing estimates.

The data in [34] allows to more than triple our dataset, compared with what we had before, leading to the possibility of a more thorough numerical analysis. First, we can achieve a better accuracy, showing that the coupling is non zero by several standard deviations. And second, we also analyzed a possible dependence of the coupling on the size of the cluster as well as on its

redshift – checking for possible evolution effects. Hence, since many more X-ray data for clusters are available than for weak lensing, we can enhance our test of the dark interaction by including X-ray clusters without the weak lensing counterpart.

We can collect all these datasets by taking each mass estimate, together with its uncertainties, and constructing a likelihood function. Our data comprises a set of 34 weak lensing, X-ray and virial mass estimates from [35–37], as well as 61 X-ray and virial (optical) mass estimates from [34]. The weak lensing and X-ray masses were compared with the optical data, and the results are represented in figure (1).

One of the difficulties, already encountered in our previous paper, is how to deal with asymmetric errors. At that time we just worked with the average error, discarding corrections due to such an asymmetry. Taking this asymmetry into account, e.g. by making use of the techniques presented in Ref. [6], may lead to more accurate constraints, however, there are some difficulties associated with the asymptotic behaviour of the likelihood function, and the final results are not significantly different from the ones obtained with a more simple analysis. Hence, we employ the simpler, symmetric treatment of the errors.

With the 61 X-ray masses mentioned above (including, of course, the optical data), as well as the earlier 34 X-ray and weak lensing masses, we can construct the likelihood function \mathcal{L} for $\bar{\zeta}$ with the full dataset:

$$\mathcal{L} \propto \prod_{i=1}^N \exp \left\{ -\frac{1}{2\sigma_i^2} \left[\frac{1-2\bar{\zeta}}{1-\bar{\zeta}/2} - f_i \right]^2 \right\} , \quad (8)$$

where f represents the mass ratios M_X/M_{vir} and M_{WL}/M_{vir} , and the errors σ are approximated by a simple geometric mean of the asymmetric uncertainties for each of the data, $\sqrt{\sigma_+\sigma_-}$. Setting a conservative prior for the values of $\bar{\zeta}$ to be flat, and between -0.3 and 0.3, we obtain the probability density function displayed in figure (1). We learn that X-ray data are more robust. The weak lensing data are more spread, though consistent with X-ray measurements [29].

The joint analysis point to:

$$\bar{\zeta} = 0.14 \pm 0.01 \quad . \quad (9)$$

Notice that the likelihood function assumes implicitly that all the variation in the mass estimations can be attributed to a single parameter, and the peak and width of that likelihood give us the best-fit and the uncertainty for that parameter. We could also have made no assumption whatsoever about the nature of these estimates, and compute the sample variance of all mass esti-

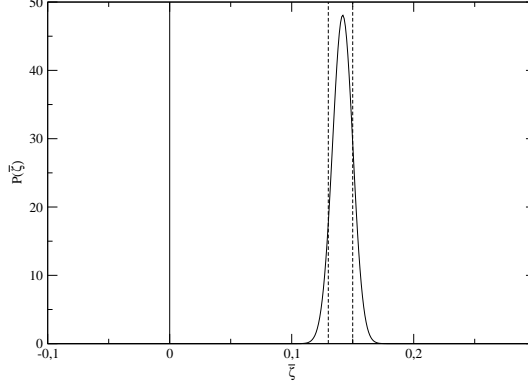


Figure 1: Probability density function (p.d.f.) for $\bar{\zeta}$ obtained with all available cluster masses. The result points to $\bar{\zeta} = 0.14 \pm 0.01$, that is, 14 standard deviations from the null result.

mates. The sample variance of the ratio between mass estimates (which is, again, degenerate with our coupling parameter) results, of course, in a much higher variance, namely $\sigma^2 = 0.3$.

The main result obtained here is that, assuming that a single parameter can explain the difference between the mass estimations, there is a positive coupling which is nonzero within several standard deviations. Now, in order to investigate whether different masses or evolution effects, for example, could be playing a role in our analysis, we can divide our data into subsets.

First, we can redo the numerical analysis after dividing the data in terms of the velocity dispersion – which is in fact a proxy for mass. This analysis leads to the three diagrams shown in figure (2).

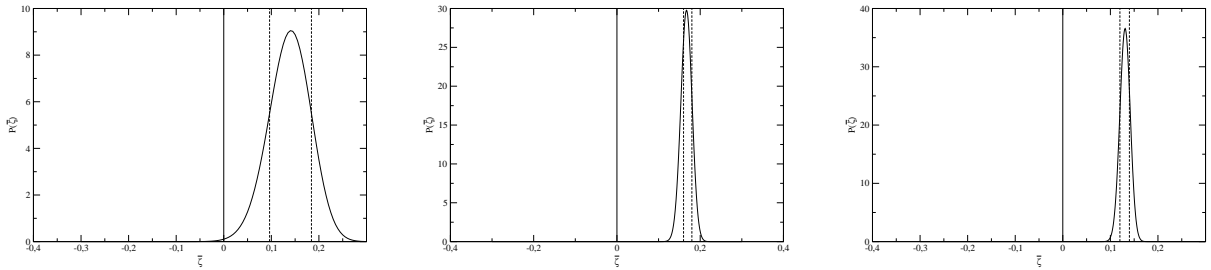


Figure 2: P.d.f's concerning the cluster data divided in three sets, in increasing order of the dispersion velocity (up to 600 km/s, from 600 to 1000 km/s, and above 1000 km/s.) The data are compatible with one another and the results point to essentially the same values of $\bar{\zeta}$, all at least three standard deviations from the null result.

The results for $\bar{\zeta}$ are, respectively, for smaller to larger values of the velocity dispersion:

$$\begin{aligned}\bar{\zeta}_{v_1} &= 0.14 \pm 0.04 \\ \bar{\zeta}_{v_2} &= 0.17 \pm 0.01 \\ \bar{\zeta}_{v_3} &= 0.13 \pm 0.01 .\end{aligned}\tag{10}$$

We can also check how robust are these results concerning the redshift – that is, we could ask whether evolution effects are important. Hence, we divide the data in subsets in order of increasing redshift – and we do this only for the X-ray observations. The results are displayed in (3).

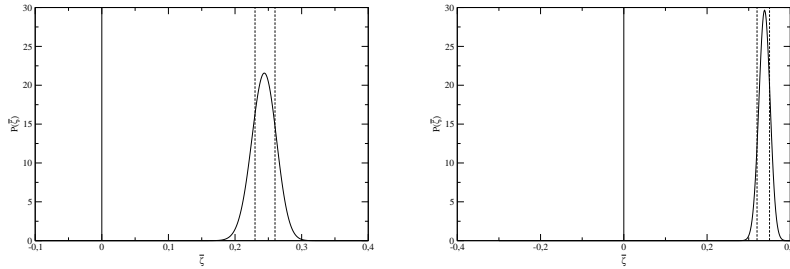


Figure 3: P.d.f's concerning the cluster data divided in two sets, in increasing order of the redshift (below and above $z = 0.05$). The data are compatible with one another and the results point to compatible values of $\bar{\zeta}$, at several standard deviations from a vanishing result. However, in the absence of weak lensing results the results point to a considerably higher value of the coupling compared with the previous ones.

The results for $\bar{\zeta}$ are, respectively, for smaller to larger values of the redshift:

$$\begin{aligned}\bar{\zeta}_{z_1} &= 0.24 \pm 0.01 \\ \bar{\zeta}_{z_2} &= 0.34 \pm 0.01 .\end{aligned}\tag{11}$$

Finally, some words are in order about choices made for the available X-ray data for cluster. Not all clusters displayed in [34] are relaxed. Moreover, some data have different results for different kinds of observations. In order to deal with these differences we used two procedures. In one, we always considered the data with largest radii. Since it is just a matter of random choice, the actual result, if robust, should not depend on it. In the second criterium, we considered the smallest radii. The results obtained using smaller and larger values of the radius are, respectively:

$$\begin{aligned}\bar{\zeta}_{r_1} &= 0.32 \pm 0.01 \\ \bar{\zeta}_{r_2} &= 0.30 \pm 0.01 .\end{aligned}\tag{12}$$

Hence, we conclude that for both criteria the results of our analysis are very similar, which means that our constraints are sufficiently robust with respect to these choices.

IV. COMPARISON WITH PREVIOUS RESULTS

In addition to the constraints obtained above, there are several other results concerning the interaction of dark energy and dark matter. A possible transition of the Dark Energy equation of state has been observed and an analysis of an explanation of such a transition in terms of Dark Energy and Dark Matter interaction in the terms proposed here has been performed in [12]. Such an analysis leads to results which can be translated to constraints in $\bar{\zeta}$ as

$$\bar{\zeta} = 0.18 \pm 0.18 \quad . \quad (13)$$

That study has been made using a holographic model for Dark Energy, but essential was the interaction between the two dark sectors.

Furthermore, a study of the age of the old quasar APM 0879 + 5255 also constrains the interaction [13]. Indeed, such a quasar is too old to be accomodated by the standard cosmology, and we have shown in [13] that an interaction leaking energy from the dark energy into dark matter sector such that the coupling constant is given by

$$\bar{\zeta} = 0.36 \pm 0.18 \quad (14)$$

naturally accomodates the age of the quasar being also compatible with the age of the universe as given by CMB observations.

On the other hand, the small ℓ behavior of the CMB angular spectrum [38] deviation from the standard model leads to further constrains in the interaction as given by [13]

$$\bar{\zeta} = 0.45 \pm 0.15 \quad . \quad (15)$$

Furthermore, the interaction can also be modeled by an alternative interacting field theory lagrangian, where Dark Energy is described by a tachyonic lagrangian while the role of dark matter is played by a fermionic field. A minimal interaction of the Yukawa type completes the picture. Such a model is constrained by baryon acoustic oscillations (BAO), lookback time, supernovae and CMB shift parameter [39]. The effective coupling of both sectors, namely fermionic (dark matter) and bosonic (dark energy) is constrained to fulfill

$$\bar{\zeta} = 0.17 \pm 0.09 \quad . \quad (16)$$

Further observational data (once again taking into account supernovae, shift parameter, BAO and galaxies ages estimates data) together with a phenomenological model based on a two fluid

interaction also points to some (feeble) constraints [40]

$$\bar{\zeta} = 0.01 \pm 0.04 \quad , \quad (17)$$

where we have considered only the most conservative result of that analysis (in fact, the results present a weak dependence on the type of interaction; we have taken the average, most conservative result).

Entirely theoretical arguments derived from a thermodynamical analysis allows an estimation of the interaction parameter for the two fluid model as [41],

$$\bar{\zeta} = 0.15 \pm 0.15 \quad . \quad (18)$$

We also recall here a previous result concerning a smaller set of clusters (contained in the total data set used in the present work): [29],

$$\bar{\zeta} = 0.04 \pm 0.02 \quad . \quad (19)$$

Our joint set of cluster observations led us to the constraint of Eq. (9). This is one way of viewing our result. However, considering the subsequent analysis (in particular the sample variance), it may be fair to see the errors as much larger, possibly of the order of magnitude of the highest difference in sub-averages. Considering the highest spread to be $\delta\bar{\zeta} = 0.5 \times (0.34 - 0.14) = 0.10$, we take our results here as:

$$\bar{\zeta} = 0.14 \pm 0.10 \quad . \quad (20)$$

Even in this pessimistic case, we can infer that our result supports the previous ones, i.e., that the interaction coupling parameter is a small but positive and of the order of 0.1, and almost three standard deviations from vanishing.

V. CONCLUSIONS

We are fully aware that our lack of precise knowledge about the errors arising from systematics could weaken our conclusions. We recall here that our main work hypothesis is that the differences between the various kinds of masses estimates come solely from the fact that they do or do not take into account the interaction parameter. Obviously, this assumption is not absolutely true, but represents an approximation we use to replace the need to analyze any particular systematic effects. Also, we have used in this work the best available data sets well-suited for our purposes.

Nevertheless, we still believe that our analysis, combined with previous results, signals in a coherent manner towards the possibility of the dark energy-dark matter interaction.

The scenario in which dark energy and dark matter are in interaction seems to be a strong physical possibility. The interaction intensity is a small constant, possibly larger than the fine structure constant, in agreement with [17]. The results are all consistent among themselves, and we obtain the interesting conclusion that the interaction constant is far from zero by several (possibly three) standard deviations, which is a rather intriguing conclusion. The positive value is also in agreement with the thermodynamical arguments of [42], strengthening our conclusions. A few words should be said about the possible influence of the interaction parameter on the cosmic history (in particular, in the structure formation process). The behavior of dark matter density as a function of time can be rather different from the non interacting case depending on the kind of interaction considered. We do not think that the proposed interaction should be the same along the whole history since decoupling, when a more robust suggestion has to be made. Since usually the matter-radiation equality is supposed to occur, in the standard model (e.g. in the non dark sector case) as well, the order of magnitude of the cosmological time parameter should not get strongly modified. (Notice that in the past, with interaction, dark matter density was smaller compared to the noninteracting case. Thus, the matter density is bounded from below by the baryonic matter density.)

Acknowledgments

This work has been supported by the Brazilian funding agencies FAPESP and CNPq. We thank an anonymous referee for useful comments.

-
- [1] A. G. Riess et al., *Astron. J.* **116** (1998) 1009; S. Perlmutter et al., *Astrophys. J.* **565** (1999) 517; P. de Bernardis et al., *Nature* **404** (2000) 955; R. Knop et al., *Astrophys. J.* **598** (2003) 102; A. G. Riess et al., *Astrophys. J.* **607** (2004) 665; P. Astier et al., *Astron. Astrophys.* **447** (2006) 31; W. M. Wood-Vasey et al., astro-ph/0701041.
 - [2] WMAP, D. N. Spergel et al., *Astrophys. J. Suppl.* **170** (2007) 377.
 - [3] SDSS, D. J. Eisenstein et al., *Astrophys. J.* **633** (2005) 560.
 - [4] T. Padmanabhan, *Phys. Rept.* **380** (2003) 235, hep-th/ 0212290; P. J. E. Peebles, B. Ratra, *Rev. Mod. Phys.* **75** (2003) 559, astro-ph/0207347; V. Sahni, *Lect. Notes Phys.* **653** (2004) 141-180, astro-ph/0403324.

- [5] L. Amendola, *Phys. Rev.* **D62**: 043511 (2000); Luca Amendola and Claudia Quercellini, *Phys. Rev.* **D68** (2003) 023514; Luca Amendola, Shinji Tsujikawa and M. Sami, *Phys. Lett.* **B632** (2006) 155-158.
- [6] R. Barlow, physics/0406120.
- [7] M. Pietroni, *Phys. Rev.* **D67** (2003) 103523; D. Comelli, M. Pietroni and A. Riotto *Phys. Lett.* **B571** (2003) 115-120.
- [8] G. Farrar and P. J. E. Peebles, *Astrophys. J.* **604** (2004) 1-11.
- [9] D. Pavon, W. Zimdahl *Phys. Lett.* **B628** (2005) 206-210, gr-qc/0505020.
- [10] S. Campo, R. Herrera, G. Olivares, D. Pavon, *Phys.Rev.* **D74** (2006) 023501; S. Campo, R. Herrera, D. Pavon, *Phys.Rev.* **D71** (2005) 123529; G. Olivares, F. Atrio- Barandela, D. Pavon, *Phys. Rev.* **D71** (2005) 063523.
- [11] G. Olivares, F. Atrio-Barandela, D. Pavon, *Phys. Rev.* **D74** (2006) 043521.
- [12] B. Wang, Y.G. Gong, E. Abdalla, *Phys. Lett.* **B624** (2005) 141; B. Wang, C.Y. Lin, E. Abdalla, *Phys.Lett.* **B637** (2006) 357.
- [13] B. Wang, J. Zang, C.Y. Lin, E. Abdalla, S. Micheletti, *Nucl. Phys.* **B778** (2007) 69-84.
- [14] S. Das, P. S. Corasaniti and J. Khoury, *Phys. Rev.* **D73** (2006) 083509.
- [15] G. Huey and B. Wandelt, *Phys. Rev.* **D74** 023519 (2006).
- [16] W. Zimdahl, *Int. J. Mod. Phys.* **D14** (2005) 2319-2326, gr-qc/0505056.
- [17] E. Abdalla and B. Wang *Phys. Lett.* **B651** (2007) 89-91.
- [18] C. Feng, B. Wang, Yungui Gong, Ru-Keng Su, *JCAP* **0709** (2007) 005, arXiv:0706.4033.
- [19] Z. K. Guo, N. Ohta and S. Tsujikawa, *Phys. Rev.* **D76** (2007) 023508, astro-ph/0702015.
- [20] P. Ferreira and M. Joyce, *Phys. Rev.* **D58** (1998) 023503.
- [21] P. Viana and A. Liddle, *Phys. Rev.* **D57** (1998) 674-684.
- [22] L. R. Abramo and F. Finelli, *Phys. Rev.* **D64** (2001) 083513.
- [23] R. Bean, *Phys. Rev.* **D 64** (2001) 123516.
- [24] N. Nunes and D. Mota, *Mon. Not. Roy. Astron. Soc.* **368** (2006) 751-758.
- [25] L. R. Abramo, R. C. Batista, L. Liberato and R. Rosenfeld, *JCAP* **0711** (2007) 012, arXiv: 0707.2882.
- [26] M. Manera and D. Mota, *Mon. Not. Roy. Astron. Soc.* **371** (2006) 1373.
- [27] P. J. E. Peebles, *Physical Cosmology* (Princeton U. Press, 1993).
- [28] O. Bertolami, F. Gil Pedro, M. Le Delliou *Gen. Rel. Grav.* arXiv:0705.3118 [astro-ph]; *Phys. Lett.* **B654** (2007) 165-169, astro-ph/0703462.
- [29] E. Abdalla, R. Abramo, L. Sodre and B. Wang *Phys. Lett.* **B673** (2009) 107-110.
- [30] Jussi Valiviita, Elisabetta Majerotto, Roy Maartens *JCAP* **0807** (2008) 020.
- [31] Jian-Hua He, Bin Wang, Elcio Abdalla *Phys. Lett.* **B671** (2009) 139-145, arXiv:0807.3471.
- [32] S. Ettori, *Mon. Not. Roy. Astron. Soc.* **344** (2003) L13.
- [33] N. Bahcall, in *Formation of Structure in the Universe*, ed. A. Dekel & J. P. Ostriker (Cambridge University Press, 1999).
- [34] M. Girardi, G. Giuricin, F. Mardirossian, M. Mezzetti, W. Boschin *Astrophys. J.* **505** (1998) 74,

astro-ph/9804187.

- [35] E. S. Cypriano, L. Sodré, J.-P. Kneib and L. E. Campusano, *Astrophys. J.* **613** (2004) 95.
- [36] E. S. Cypriano, G. B. Lima Neto, L. Sodré, J.-P. Kneib and L. E. Campusano, *Astrophys. J.* **630** (2005) 38.
- [37] H. Hoekstra, *Mon. Not. Roy. Astron. Soc.* **379** (2007) 317.
- [38] Zuo-Yi Huang, Bin Wang, Elcio Abdalla, Ru-Keng Su *JCAP* **0605** (2006) 013, e-Print: hep-th/0501059; Jian-yong Shen, Bin Wang, Elcio Abdalla, Ru-Keng Su *Phys. Lett.* **B609** (2005) 200-205, e-Print: hep-th/0412227.
- [39] Sandro Micheletti, Elcio Abdalla, Bin Wang *Phys. Rev.* **D79** (2009) 123506 arXiv:0902.0318.
- [40] Chang Feng, Bin Wang, Elcio Abdalla, Ru-Keng Su *Phys. Lett.* **B665** (2008) 111-119, arXiv:0804.0110.
- [41] Bin Wang, Chi-Yong Lin, Diego Pavon, Elcio Abdalla *Phys. Lett.* **B662** (2008) 1-6, arXiv:0711.2214.
- [42] Diego Pavon, Bin Wang *Gen. Rel. Grav.* **41** (2009) 1-5, arXiv:0712.0565.